The electronic structure of $Al_yGa_xIn_{1-x-y}As$ alloys and related heterojunctions

1997 J. Phys.: Condens. Matter 9 3151

(http://iopscience.iop.org/0953-8984/9/15/008)

J. Phys.: Condens. Matter **9** (1997) 3151–3162. Printed in the UK PII: S0953-8984(97)76736-5

The electronic structure of $Al_yGa_xIn_{1-x-y}As$ alloys and related heterojunctions

San-Guo Shen†‡ and Xi-Qing Fan‡

† China Centre of Advanced Science and Technology (World Laboratory), PO Box 8730, Beijing, 100080, People's Republic of China

‡ Physics and Engineering College, Zhengzhou University, Zhengzhou 450052, People's Republic of China

Received 30 July 1996, in final form 10 December 1996

Abstract. The dependences on composition of the bond lengths and energy bands of $Al_yGa_xIn_{1-x-y}As$ quaternary alloys are calculated on the basis of tight-binding theory under the virtual-crystal approximation. For a $Al_yGa_xIn_{1-x-y}As$ quaternary alloy lattice matched to InP, a type II staggered band line-up is observed when the Al composition is larger than 24%. At this point the conduction band discontinuity of $Al_yGa_xIn_{1-x-y}As/InP$ heterostructures disappears. The effective electron mass associated with the conduction band minimum is estimated on the basis of the $\boldsymbol{k}\cdot\boldsymbol{p}$ theory, and is in good agreement with the cyclotron resonance experimental results. The relative conduction band discontinuity $\Delta E_c/\Delta E_g$ is determined to be 72.2% for $In_{0.53}Ga_{0.47}As/In_{0.52}Al_{0.48}As$. The band offsets of the related heterojunctions are calculated, and compared with experimental and previous theoretical results.

1. Introduction

The $Al_yGa_xIn_{1-x-y}As$ alloy material system lattice matched to InP is easily prepared by molecular beam epitaxy (MBE). It has long found applications in optical communication devices such as emitters, waveguides, and detectors [1, 2], and is ideal for heterojunction bipolar transistors and high-mobility field-effect transistors [3]. $In_{0.53}Ga_{0.47}As/In_{0.52}Al_{0.48}As$ heterostructures lattice matched to InP are particularly attractive for high-performance electronic and photonic devices as well as for future optoelectronic integrated circuits, because of the large difference of band gaps. The physical properties of the alloy and heterostructures have been investigated in great detail.

The band gap and electron effective mass of $Al_yGa_xIn_{1-x-y}As$ lattice matched to InP have been measured by photoluminescence (PL) [4–6] and cyclotron resonance (CR) [4, 5] experiments.

In this work the study of the electronic structure of $Al_yGa_xIn_{1-x-y}As$ on the basis of the tight-binding method is carried out. The local atomic structure is obtained on the basis of the bond-orbital model (BOM). The bond lengths d_{AlAs}, d_{GaAs}, d_{InAs}, and $d_{average}$ in $Al_yGa_xIn_{1-x-y}As$ versus the composition x and y are calculated. Using the Slater–Koster Hamiltonian with the simple virtual-crystal approximation (VCA), the dependences on the composition of the energy bands and band offsets are calculated. Also the electron effective mass versus composition x is estimated on the basis of the $\boldsymbol{k}\cdot\boldsymbol{p}$ theory. The results are compared with experimental and other theoretical results.

The paper is organized as follows. Section 2 describes the method used for the present calculation. The results will be presented in section 3, followed by a discussion and

0953-8984/97/153151+12$19.50

comparison with available experiments. A brief summary of our conclusions is contained in section 4.

2. Theoretical formalism

2.1. Bond-length relaxation

The local atomic structure, and impurity–host relaxation in semiconductors can be obtained on the basis of the tight-binding BOM [7]. In the notation of Harrison [8], the gain in the impurity–host bond energy per bond connected with a distortion Δd ($\Delta d > 0$ outward and $\Delta d < 0$ inward) can be calculated as follows:

$$\Delta E_b = \Delta E_b^1 + 3\,\Delta E_b^2 \tag{1}$$

where ΔE_b^1 and ΔE_b^2 are, respectively, the changes in the energies of the bonds caused by distortion in the nearest- and second-nearest-neighbour atom positions. These are given by

$$\begin{aligned}\Delta E_b^1 = -2\{&[V_2^2(d_0+\Delta d)+V_3^2]^{1/2} - V_2^2(d_0+\Delta d)/k|\bar{\varepsilon}_h| \\ &- [V_2^2(d_0)+V_3^2]^{1/2} + V_2^2(d_0)/k|\bar{\varepsilon}_h|\}\end{aligned} \tag{2}$$

and

$$\begin{aligned}\Delta E_b^2 = -2\{&[V_2'^2(d_0+\Delta d')+V_3'^2]^{1/2} - V_2'^2(d_0+\Delta d')/k'|\overline{\varepsilon'}_h| \\ &- [V_2'^2(d_0)+V_3'^2]^{1/2} + V_2'^2(d_0)/k'|\overline{\varepsilon'}_h|\}\end{aligned} \tag{3}$$

where d_0 is the bond length of the host crystal, and V_2, V_3, and $k|\bar{\varepsilon}_h|$ refer to the covalent and polar bond energies and the average hybrid energy of the impurity nearest-neighbour bond, respectively.

V_2 is the hybrid covalent energy, which can be approximated in the following way:

$$V_2 = -\eta_\sigma \frac{\bar{h}^2}{md^2} \tag{4}$$

where, for sp^3 bonds, $\eta_\sigma = \frac{1}{4}\eta_{ss\sigma} - (\sqrt{3}/2)\eta_{sp\sigma} - \frac{3}{4}\eta_{pp\sigma}$, in which $\eta_{ss\sigma} = -1.4$, $\eta_{sp\sigma} = 1.84$ and $\eta_{pp\sigma} = 3.24$ are dimensionless Harrison universal parameters, and $\bar{h}^2/m = 7.62$ eV Å^2. V_3 is the hybrid polar energy, which can be approximated in the following way:

$$V_3 = \frac{1}{2}(\varepsilon_h^c - \varepsilon_h^a) \tag{5}$$

where ε_h^c and ε_h^a are the cation and anion hybrid energy where for sp^3 bonds

$$\varepsilon_h^c = \frac{1}{4}(\varepsilon_s^c + 3\varepsilon_p^c) \qquad \varepsilon_h^a = \frac{1}{4}(\varepsilon_s^a + 3\varepsilon_p^a) \tag{6}$$

in which ε_s^c, ε_p^c, ε_s^a, and ε_p^a, are the energies for s and p states for the cation and anion in the solid, respectively. These values could differ somewhat from the corresponding values defined for the free atom; following Harrison [8], we will use free-atom values. The effective parameter k will be given by the following average:

$$k = \sqrt{k_i k_j} \tag{7}$$

where k_i and k_j are connected with rows i and j, respectively, of the periodic table [7]. The cation–anion average hybrid energy $\bar{\varepsilon}_h$ is the weighted average

$$\bar{\varepsilon}_h = \frac{1}{8}(n_c\varepsilon_h^c + n_a\varepsilon_h^a) \tag{8}$$

where n_c and n_a are the numbers of electrons associated with the cation and anion, respectively, which participate in the bonds. $\Delta d'$ is the change in the bond length between the first- and second-nearest neighbours. If we hold the second-nearest neighbours fixed, the following formula can be obtained:

$$\Delta d' = \sqrt{d_0^2 - \frac{2}{3}d_0\,\Delta d + (\Delta d)^2} - d_0. \tag{9}$$

Under the first-order approximation, $\Delta d' = -\frac{1}{3}\Delta d$. The terms V_2', V_3', and $k'|\overline{\varepsilon'}_h|$ are the covalent and polar bond energies, and average hybrid energy of the host crystal, respectively. Within this approximation the minimum of the total energy predicates the impurity–host relaxation.

2.2. Band structure

The energy band structure of $Al_yGa_xIn_{1-x-y}As$ is described by use of the tight-binding Slater–Koster [9] Hamiltonian of binaries in the VCA. Following Harrison [8], the weighted-average tight-binding parameters p_i for the alloy crystal including the on-site matrix elements and the second-neighbour parameters are linearly interpolated as a function of x and y, i.e.,

$$p_i(Al_yGa_xIn_{1-x-y}As) = yp_i(AlAs) + xp_i(GaAs) + (1-x-y)p_i(InAs). \tag{10}$$

Considering the dependence of p_i on the bond length in $Al_yGa_xIn_{1-x-y}As$, the nearest-neighbour off-diagonal matrix elements can be obtained from

$$\begin{aligned} d^2(x,y)p_i(Al_yGa_xIn_{1-x-y}As) &= d^2_{AlAs}(x,y)yp_i(AlAs) \\ &\quad + d^2_{GaAs}(x,y)xp_i(GaAs) + d^2_{InAs}(x,y)(1-x-y)p_i(InAs) \end{aligned} \tag{11}$$

where $d_{AlAs}(x,y)$, $d_{GaAs}(x,y)$, $d_{InAs}(x,y)$, and $d(x,y)$ are the bond lengths of AlAs, GaAs, InAs, and the average bond length in $Al_yGa_xIn_{1-x-y}As$, respectively, and

$$d(x,y) = yd_{AlAs}(x,y) + xd_{GaAs}(x,y) + (1-x-y)d_{InAs}(x,y). \tag{12}$$

These assumptions leave the symmetry of the alloy unchanged, i.e., the tetrahedral structure remains. Since there is little bowing in the fundamental band edge of the ternary alloys $Al_yGa_{1-y}As$ [10], $Al_yIn_{1-y}As$ [11], and $Ga_xIn_{1-x}As$ [12], the above approximations are known to be quite reasonable for $x+y=1$, $x=0$, or $y=0$, respectively, for $Al_yGa_xIn_{1-x-y}As$. So the assumptions might be suitable for $Al_yGa_xIn_{1-x-y}As$.

2.3. Effective mass

The $\boldsymbol{k}\cdot\boldsymbol{p}$ perturbation theory gives the expressions for energies and wave functions near a semiconductor band extremum. The effective mass is inversely proportional to the energy band curvature. For a conduction electron at $\boldsymbol{k}=0$ in a cubic semiconductor, the effective mass is expressed as [13]

$$\frac{m_0}{m^*} - 1 = \frac{P^2}{3}\left(\frac{2}{E_0} + \frac{1}{E_0+\Delta_0}\right) - \frac{P'^2}{3}\left(\frac{2}{E(\Gamma_8^c)-E_0} + \frac{1}{E(\Gamma_7^c)-E_0}\right) + C \tag{13}$$

in which E_0 is the Γ_8^v–Γ_6^c gap, and Δ_0 the valence band spin–orbit splitting. P is the momentum matrix element connecting the p-type valence band with the s-type conduction band, and P' is the momentum matrix element connecting the s-type conduction band with the next higher-lying p-type conduction band. C is a small correction for all higher-lying bands. Because the conduction and valence band wavefunctions differ on going from GaAs

to AlAs and InAs, in order to calculate the effective mass of $Al_yGa_xIn_{1-x-y}As$, it must be expected that P and/or P' will also vary with the Al and Ga contents x and y.

3. Results and discussion

In this section we present the results of our tight-binding calculation for the bond lengths, the electronic band structure, and band offsets as functions of the compositions x and y in $Al_yGa_xIn_{1-x-y}As$ alloys. The results for the alloys lattice matched to InP are compared with the available experimental results.

3.1. Bond lengths

The bond lengths around the impurity for the six systems AlAs:Ga and AlAs:In, GaAs:Al and GaAs:In, and InAs:Al and InAs:Ga are obtained from equations (1)–(3) on the basis of the BOM. The lattice relaxations (Δd) are -0.002 and 0.126, 0.002 and 0.127, -0.134 and -0.138 Å, respectively.

Table 1. Bond lengths (in Å) for $A_xB_{1-x}C$.

Alloys	$d_{AC}(x=0)$	$d_{AC}(x=1)$	$d_{BC}(x=0)$	$d_{BC}(x=1)$	References
$Ga_xAl_{1-x}As$	2.449	2.448	2.451	2.450	This work
	2.449	2.448	2.451	2.450	[16]
$Ga_xIn_{1-x}As$	2.485	2.448	2.623	2.575	This work
	2.486	2.448	2.623	2.562	[16]
	2.495	2.448	2.622	2.556	[15]
	2.487	2.448	2.623	2.586	[14]
$Al_xIn_{1-x}As$	2.489	2.451	2.623	2.577	This work
	2.488	2.451	2.623	2.562	[16]
	2.495	2.451	2.622	2.553	[15]

According to our calculation, the bond lengths of GaAs and InAs in $Ga_xIn_{1-x}As$ alloys in the dilute limits ($x \to 0$ or $x \to 1$) are 2.485 and 2.575 Å, respectively. The experimental results are available for $Ga_xIn_{1-x}As$; the bond lengths of GaAs and InAs in the dilute limits measured using extended x-ray absorption fine structure (EXAFS) are 2.487 and 2.586 Å [14], respectively. Martins and Zunger [15] have calculated the bond lengths in crystalline $Ga_xIn_{1-x}As$ alloys using a valence force-field (VFF) model, and the bond lengths of GaAs and InAs in the dilute limit are 2.495 and 2.556 Å. The effective-medium approximation (EMA) has been used by Cai and Thorpe [16] to calculate the bond lengths in crystalline $Ga_xIn_{1-x}As$ alloys, and the bond lengths of GaAs and InAs in the dilute limit are 2.486 and 2.562 Å. The available results for $Ga_xIn_{1-x}As$, $Ga_xAl_{1-x}As$ and $Al_xIn_{1-x}As$ alloys are shown in table 1. It is clear that a serious discrepancy exists between the VFF [15] calculation and the EXAFS analysis. Our results are in good agreement with the EMA results and closer to the results obtained from the EXAFS experiment for $Ga_xIn_{1-x}As$.

In order to describe the bond-length relaxation, Martins and Zunger [15] defined a dimensionless relaxation parameter $\xi = (d_0^{BC}[\text{AC:B}] - d_0^{AC})/(d_0^{BC} - d_0^{AC})$. According to our BOM calculation, the values of ξ for GaAs and InAs bonds in $Ga_xIn_{1-x}As$ are about 0.79 and 0.73. The EXAFS experimental results are about 0.78 and 0.79, and the VFF results are about 0.73 and 0.62. So our results are closer to the experimental results for $Ga_xIn_{1-x}As$ alloys.

It is clear from the EXAFS experiment [14] that the relationship between the bond lengths $d_{GaAs}(x)$ and $d_{InAs}(x)$ of $Ga_xIn_{1-x}As$ alloys and the composition is nearly linear. So our model for the dilute alloy can be extended to the whole range of composition by a linear interpolation of the data for the end-point materials. The results for the AlAs, GaAs, and InAs bond lengths in $Al_yGa_xIn_{1-x-y}As$ alloys are given by

$$\begin{aligned} d_{AlAs}(x, y) &= 2.450x + 2.451y + 2.489(1 - x - y) \\ d_{GaAs}(x, y) &= 2.448x + 2.449y + 2.485(1 - x - y) \\ d_{InAs}(x, y) &= 2.575x + 2.577y + 2.623(1 - x - y). \end{aligned} \tag{14}$$

The bond lengths of AlAs are in the range 2.450 to 2.489 Å, and the bond lengths of GaAs are in the range 2.448 to 2.485 Å, while the bond lengths of InAs are in the range 2.575 to 2.623 Å. Therefore, the AlAs, GaAs, and InAs bond lengths in alloys tend to maintain their respective lengths: nearly 2.451 Å for the AlAs bond, 2.448 Å for the GaAs bond, and 2.623 Å for the InAs bond. The largest relative deviations of bond lengths in alloys from the bond lengths in their compounds are about 1.6%, 1.5%, and 1.8%, respectively.

The average bond length of $Al_yGa_xIn_{1-x-y}As$ alloys can be obtained from the weighted-average bond length over $d_{AlAs}(x, y)$, $d_{GaAs}(x, y)$, and $d_{InAs}(x, y)$. We find that $d(x, y)$ varies monotonically, and nearly follows Vegard's law (our result has a very small negative deviation of -0.01% at $x = 0.5$ from Vegard's law). Contours of the constant bond lengths in $Al_yGa_xIn_{1-x-y}As$ alloys are shown in figure 1. From figure 1, some qualitative features can be summarized.

(1) The amount of change in each bond length is rather small, i.e., the bond length does not deviate much from that in the corresponding binary compound.

(2) The equal-bond-length lines in figures 1(a)–1(c) are parallel to those in figure 1(d); thus the length of each bond barely depends on the composition if the average bond length is a constant. So for the quaternary alloy lattice (average bond length) matched to InP, the bond lengths of AlAs, GaAs, and InAs in alloys will be constants.

(3) When $x + y$ is a constant, the lengths of the four bonds are nearly constants. For example, when $x + y = 0.47$, the average bond length of the quaternary alloy is about 2.54 Å, i.e., if lattice matched to InP, the bond lengths of AlAs, GaAs, and InAs are about 2.471, 2.468, and 2.600 Å, respectively.

(4) For all four bonds, the spacing between equal-bond-length lines becomes wide when the Al and Ga contents are large, and thus the bond-length distortion increases as the In content increases. This deviation is caused by the difference in the dimensionless relaxation parameter.

The bond lengths $d_{AlAs}(x, y)$, $d_{GaAs}(x, y)$, $d_{InAs}(x, y)$, and $d(x, y)$ will be used to calculate the electronic band structure.

3.2. Electronic band structures and offsets

The band structures of AlAs, GaAs, and InAs have been calculated by several methods, the results being in general agreement. However, because in most of these the energy zero is set to the valence band top, we cannot obtain the band offset from them.

Here, the electronic structure is calculated using a tight-binding model with the interaction range restricted to second-nearest neighbours. The parameters in the Hamiltonian matrix for AlAs, GaAs, and InAs are given by Wilke and Hennig [17]; the energy zero is set to the valence band top for GaAs, so we can use these parameters to obtain the band offset. However, for InAs, the band gap given by reference [17] is 0.573 eV, but the experimental

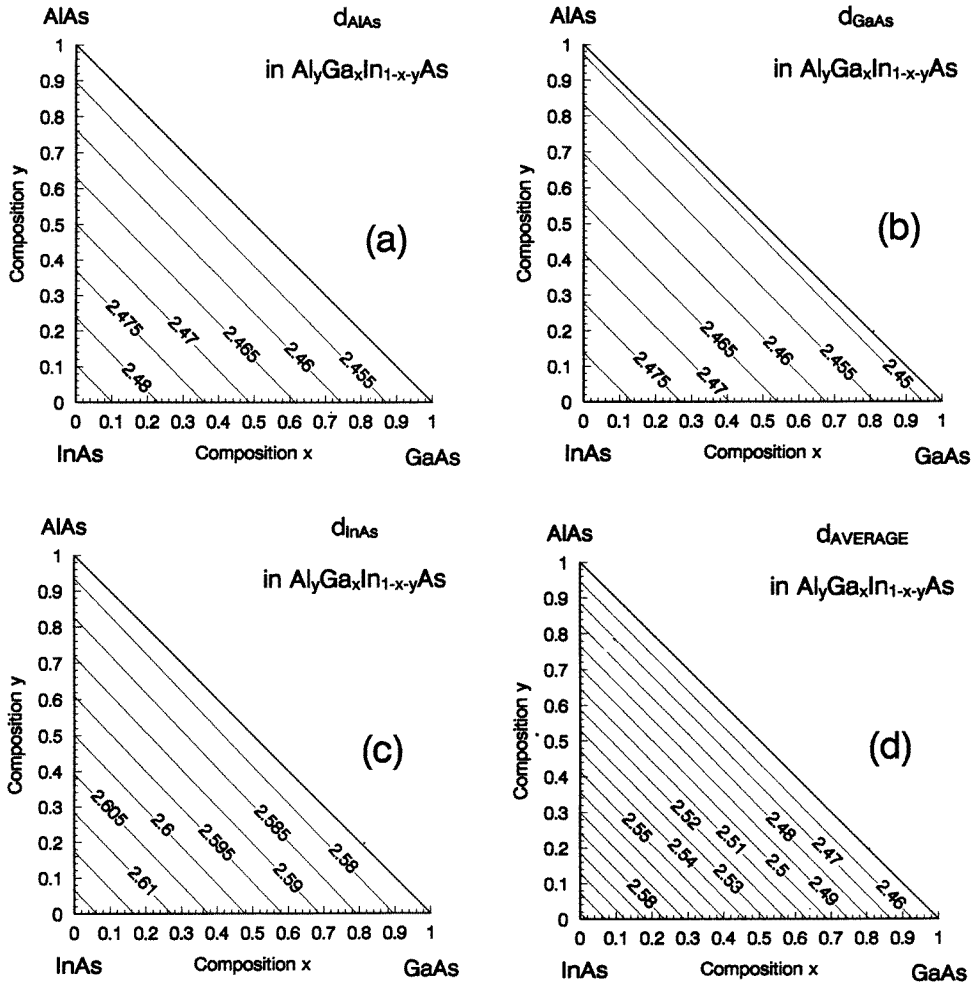

Figure 1. Contours of the constant bond lengths (in Å) in $Al_yGa_xIn_{1-x-y}As$ alloys.

result is 0.418 eV [18]. Because the band gap of InAs is very important for the band gap of the quaternary alloy, we should adjust the values of the interaction parameters of reference [17] so as to obtain agreement with the band gap of the experiment. During the adjustment procedure, we hold the lowest conduction band energy fixed, i.e., the conduction band offset between InAs and GaAs is taken to be the same as in reference [17] (0.79 eV); attention is paid to obtaining a good description of the upper valence band.

For quaternary $Al_yGa_xIn_{1-x-y}As$ alloys, the Hamiltonian is obtained using the VCA as in equations (10)–(12) and (14). The alloy Hamiltonian is diagonalized to give the band structure, and then the band offset can be obtained from the band structure directly.

The values for the band gaps of AlAs, GaAs, InAs, and InP, and the valence band offsets ΔE_v, conduction band offsets ΔE_c, and band-gap offsets ΔE_g for GaAs/AlAs, GaAs/InAs, InAs/AlAs, and InP/GaAs are listed in table 2, in which the band gaps of AlAs, GaAs, and InAs, and the band offsets for GaAs/AlAs, GaAs/InAs, and InAs/AlAs are obtained directly from our energy band calculation. The band gap of InP is taken to be the experimental

Table 2. The values (eV) of the band gaps of AlAs, GaAs, InAs, and InP, and the valence band offsets ΔE_v, conduction band offsets ΔE_c, and band-gap offsets ΔE_g for GaAs/AlAs, GaAs/InAs, InAs/AlAs, and InP/GaAs heterojunctions. $\Delta E_v > 0$ for A/B heterojunctions means $E_v(\mathrm{B}) > E_v(\mathrm{A})$; $\Delta E_c > 0$ means $E_c(\mathrm{B}) > E_c(\mathrm{A})$.

Compounds	E_g	Heterojunctions	ΔE_v	ΔE_c	ΔE_g
AlAs	2.267	AlAs/GaAs	0.556	−0.200	−0.756
GaAs	1.511	GaAs/InAs	0.301	−0.792	−1.093
InAs	0.418	InAs/AlAs	−0.857	0.992	1.849
InP	1.423	InP/GaAs	0.110	0.198	0.088

result [19], and the valence band offset of InP/GaAs is obtained by means of Harrison's method [20], and the conduction band offset is obtained from $\Delta E_c = \Delta E_g + \Delta E_v$. The valence band offset of GaAs/InAs is 0.301 eV, which is in good agreement with the result of 0.32 eV obtained by Harrison's method [20].

The AlAs/GaAs heterostructure is different from GaAs/InAs in which the conduction band minimum of AlAs is near the X point of the Brillouin zone. The valence band offset of AlAs/GaAs is 0.556 eV; it is in good agreement with the recently measured results 0.55 eV [21] and 0.586 ± 0.015 eV [22]. Many first-principles calculations of the valence band offset for AlAs/GaAs can be found in the literature. The result obtained from the atomic-sphere approximation (ASA) of the linear muffin-tin orbital (LMTO) method is 0.53 eV [23]. The result obtained by the self-consistent dipole profile (SCDP) method is 0.54 eV [24].

Table 3. Valence band offsets (in eV) for $Ga_xAl_{1-x}As/GaAs$. ΔE_v^1 are the experimental results [21], ΔE_v^2 are our results, and ΔE_v^3 are LMTO-ASA results [26].

Al composition	ΔE_v^1	ΔE_v^2	ΔE_v^3	$\Delta E_v^1 - \Delta E_v^2$	$\Delta E_v^1 - \Delta E_v^3$
0.25	0.145	0.121	0.133	0.024	0.012
0.36	0.185	0.178	0.191	0.007	−0.006
0.38	0.190	0.188	0.202	0.002	−0.012
0.60	0.335	0.311	0.319	0.024	0.016
0.74	0.420	0.393	0.393	0.027	0.027
1.00	0.550	0.556	0.532	−0.006	0.018

The band alignment in $Ga_xAl_{1-x}As/GaAs$ heterostructures had been investigated over the whole range of alloy composition [21]; the valence band offsets ΔE_v were determined to be 0.145, 0.185, 0.190, 0.335, 0.420, and 0.550 eV for the Al contents $1 - x = 0.25$, 0.36, 0.38, 0.60, 0.74, and 1, respectively. These results are shown in table 3.

From our calculation of the band structure of $Ga_xAl_{1-x}As$, the offsets are 0.121, 0.178, 0.188, 0.311, 0.393, and 0.556 eV, respectively. For comparison, our results are also given in table 3. The largest deviation of our results from the experimental results [21] is less than 0.027 eV, so our results are in good agreement with the experimental results for the whole range of alloy composition.

The results of first-principles virtual-crystal calculations of the band structures of $Ga_xAl_{1-x}As$ disordered alloys and the valence and conduction band offsets of $Ga_xAl_{1-x}As/GaAs(100)$ heterostructures were given by Nelson *et al* [25]; the valence band offsets for Al contents $1 - x = 0.2$, 0.4, 0.6, 0.8, and 1.0 are 0.04, 0.17, 0.23, 0.30, and 0.40 eV, respectively. It is clear that the experimental and calculated deviations are much larger than ours.

The band structures of ordered $Ga_xAl_{1-x}As$ alloys have been studied most recently by the LMTO-ASA method, on the basis of average-bond-energy theory; Wang and Zheng [26] have determined the variations of the valence band offset $\Delta E_v(x)$ with the composition x of $Ga_xAl_{1-x}As/GaAs$ to be $\Delta E_v(x) = 0.531(1-x) + 0.001(1-x)^2$. The results are in good agreement with the experimental results $\Delta E_v(x) \simeq 0.55(1-x)$ [21]. It is clear from table 3 that our results are also in good agreement with the LMTO-ASA results [26]. So the results given below for quaternary alloys should be reasonable.

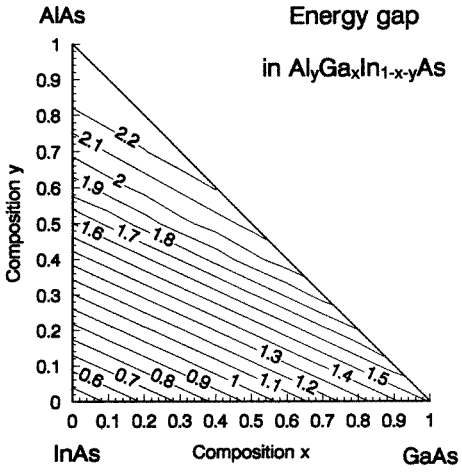

Figure 2. Contours of the constant band gaps (in eV) in $Al_yGa_xIn_{1-x-y}As$ alloys.

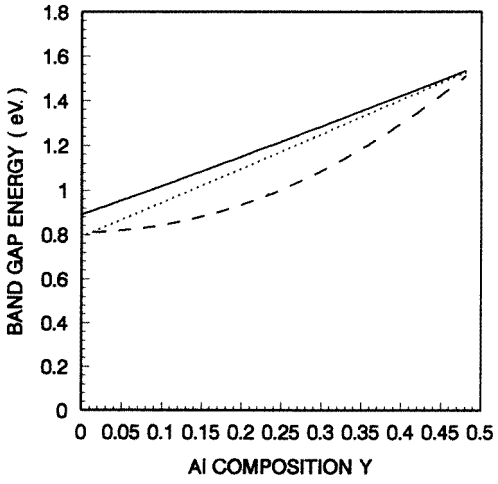

Figure 3. The energy band gap for the alloys lattice matched to InP. The dotted line is the measured result from [4]. The dashed line is the measured result from [6]. The solid line represents our result.

For quaternary alloys, contours of the constant band gaps are shown in figure 2. Results for $E_g(x, y)$ follow an almost linear dependence on composition. As an example, the

theoretical and experimental [4, 6] concentration dependence of the energy band gap for the quaternary $Al_yGa_xIn_{1-x-y}As$ alloys lattice matched to InP are shown in figure 3. To a good approximation our results from a direct calculation of E_g are described by $E_\Gamma = 0.894 + 1.296y + 0.125y^2$ (the solid line). The agreement between our calculations and experiment (the dotted line) [4] was satisfactory. However, the trend in the change of the energy band gap is different from the result of reference [6] (the dashed line).

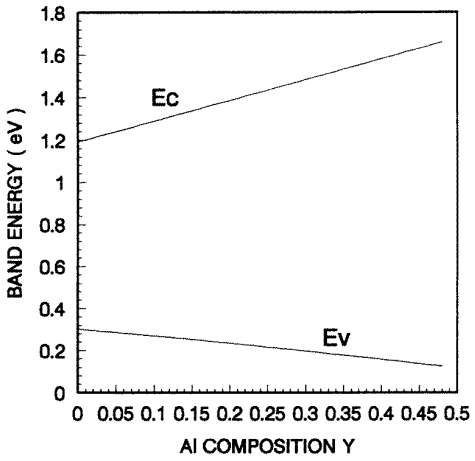

Figure 4. The conduction band edge and valence band edge as functions of Al composition y in $Al_yGa_xIn_{1-x-y}As$ lattice matched to InP. Here the zero of energy is taken to be the top of the valence band edge of InP.

The conduction band edge and valence band edge as functions of the Al content y in $Al_yGa_xIn_{1-x-y}As$ lattice matched to InP are given in figure 4. Here the zero of energy is taken to be the top of the valence band edge of InP. The valence and conduction band offsets of $Al_{0.48}In_{0.52}As$/InP are -0.119 and -0.242 eV, respectively. The result for the conduction band offset is in good agreement with the result of -0.252 eV [27]. For $Ga_{0.47}In_{0.53}As$/InP, the valence and conduction band offsets are -0.300 and 0.229 eV. The result for the conduction band offset is in good agreement with the result of 0.245 eV [28]. The variation of $\Delta E_v(y)$ and $\Delta E_c(y)$ with the Al composition can be described by $\Delta E_v(y) = -0.300 + 0.321y + 0.116y^2$ eV, and $\Delta E_c(y) = 0.229 - 0.975y - 0.010y^2$ eV ($0 \leqslant y \leqslant 0.48$), respectively. Three different fields for the band-gap alignment at the $Al_yGa_xIn_{1-x-y}As$/InP heterojunction can be distinguished as a function of the Al composition as follows.

(1) ($y \geqslant 0.41$)—the band gap of $Al_yGa_xIn_{1-x-y}As$ is larger than that of InP, and a type II band line-up exists.

(2) ($0.24 \leqslant y < 0.41$)—the band gap of $Al_yGa_xIn_{1-x-y}As$ is smaller than that of InP, but still a type II band line-up exists.

(3) ($y < 0.24$)—the band gap of $Al_yGa_xIn_{1-x-y}As$ is smaller than that of InP, and a type I band line-up exists.

These features are similar to the results determined by low-temperature photoluminescence measurements [6]: for Al compositions larger than $22\% \pm 2\%$ a type II staggered band line-up is observed, and for $y > 0.45$ the band gap of $Al_yGa_xIn_{1-x-y}As$ is larger than that of InP.

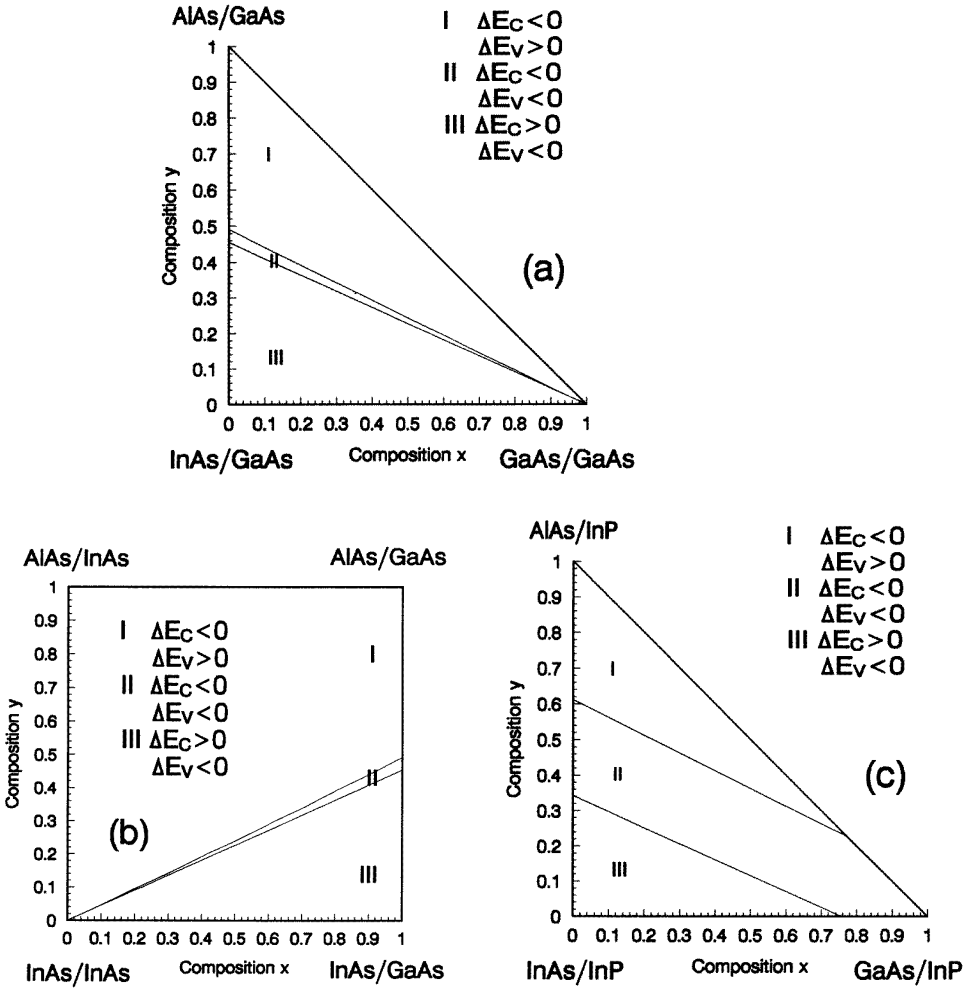

Figure 5. The regions of realization of type I and type II superlattices in the compounds $Al_yGa_xIn_{1-x-y}As/Ga_xIn_{1-x}As$ and $Al_yGa_xIn_{1-x-y}As/InP$.

The significant difference between the experimental and our theoretical results is that the experiment results for both the band gap of $Al_yGa_xIn_{1-x-y}As$ and the conduction band discontinuity between $Al_yGa_xIn_{1-x-y}As$ and InP show a quadratic dependence on Al composition, but the relationship of our results is nearly linear.

The valence and conduction band offsets of the $Al_{0.48}In_{0.52}As/Ga_{0.47}In_{0.53}As$ heterostructure are 0.181 and -0.471 eV, and $\Delta E_c \approx 0.722\Delta E_g$. They are in good agreement with the previous result: 0.196 and -0.504 eV, and $\Delta E_c \approx 0.72\Delta E_g$ [27].

The heterojunctions $Al_yIn_{1-y}As/GaAs$ are of special interest because in the range of composition $0.49 > y > 0.46$, type II superlattices are realized. Outside this range, type I superlattices are obtained. In the heterojunctions $Ga_xIn_{1-x}As/AlAs$ and $Al_yGa_{1-y}As/InAs$, only type I superlattices are realized. In the heterojunctions $Al_yIn_{1-y}As/Ga_xIn_{1-x}As$ in the region between $y = 0.46x$ and $y = 0.49x$, type II superlattices are realized. Outside this range, type I superlattices are obtained. Also, the heterojunctions $Al_yGa_xIn_{1-x-y}As/InP$ are

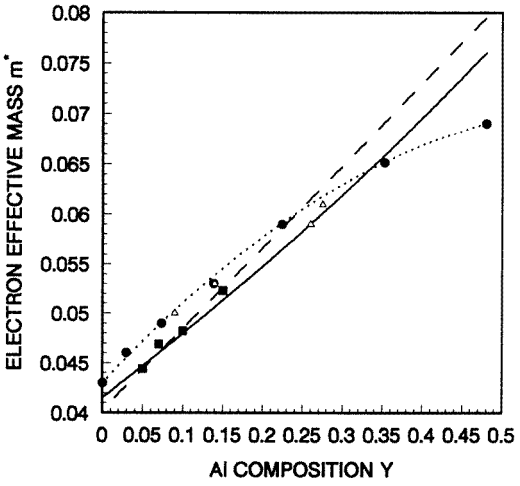

Figure 6. Values for the effective mass in $Al_yGa_xIn_{1-x-y}As$ lattice matched to InP. The dashed line is the result of the linear fit to the experimental points (solid squares) [4]. The triangles are taken from reference [32]. The dotted line is the experimental result (circles) of reference [5]. The solid line represents the $\boldsymbol{k}\cdot\boldsymbol{p}$ theory result.

of special interest because in the zone between $y = 0.34 - 0.44x$, and $y = 0.61 - 0.44x$, type II superlattices are realized. Outside this range, type I superlattices are obtained. All of the interesting results are given in figure 5.

3.3. Effective mass

For $Al_yGa_xIn_{1-x-y}As$ alloys lattice matched to InP, we assume a linear variation of the spin–orbit splitting Δ_0 and Δ_0' with x, and $\Delta_0 = 0.47 \times 0.341 + 0.53 \times 0.38 - 0.086x$ (eV), $\Delta_0' = 0.171$ (eV) [29, 30]. We use the relationship: $E(\Gamma_7^c) = E(\Gamma_5^c) - \Delta_0'/2$ and $E(\Gamma_8^c) = E(\Gamma_5^c) + \Delta_0'/2$. The interband matrix element P^2 is slightly dependent on x, and is taken to be a linear function of x [31]: $P^2 = 0.47 \times 28.9 + 0.53 \times 22.2 - 2x$ (eV). $P'^2 = 6$ eV and $C = -2$ are assumed to be constants.

The calculated effective-mass m^*-values for the alloy composition range investigated are plotted in figure 6 (the solid line). We note that the agreement with the mass dependence obtained from the cyclotron resonance experiments (squares [4] and triangles [32]) is very satisfactory. In figure 6, the dashed line is the best linear fit to $m^* = 0.0403 + 0.0817y$ (m_0) [4] obtained from the experimental data [4]. Our result can be given by $m^* = 0.0415 + 0.070y + 0.0086y^2$ (m_0). Our result for the trend in the change of the effective mass is different from the experimental result of reference [5].

4. Conclusion

The tight-binding bond-orbital model is used to predict the AlAs, GaAs, and InAs bond lengths in $Al_yGa_xIn_{1-x-y}As$ alloys. The average bond length nearly follows Vegard's law, but has a small, negative deviation. The AlAs, GaAs, and InAs lengths are close to the Pauling limit, but are dependent on composition.

The electronic band structure of $Al_yGa_xIn_{1-x-y}As$ alloys is obtained. The band offset

of the alloys and related heterojunctions are discussed. The direct-band-gap energy of the alloys lattice matched to InP is in good agreement with the photoluminescence measurement data. The effective electron mass associated with the conduction band minimum obtained from the $\boldsymbol{k} \cdot \boldsymbol{p}$ theory is compared with the cyclotron resonance experimental results.

References

[1] Olego D, Chang T Y, Silberg E, Caridi E A and Pinczuk A 1982 *Appl. Phys. Lett.* **41** 476
[2] Fujii T, Nakata Y, Sugiyama Y and Hiyamizu S 1986 *Japan. J. Appl. Phys.* **25** L254
[3] Hiyamizu, Fujii T, Muto S, Inata T, Nakata Y, Sugiyama Y and Sasa A 1987 *J. Cryst. Growth* **81** 349
[4] Kopt R F, Wei H P, Perley A P and Livescu G 1992 *Appl. Phys. Lett.* **60** 2386
[5] Cury L A, Beerens J and Praseuth J P 1993 *Appl. Phys. Lett.* **63** 1804
[6] Böhrer J, Krost A and Bimberg D B 1993 *Appl. Phys. Lett.* **63** 1918
[7] Baranowski J M 1984 *J. Phys. C: Solid State Phys.* **17** 6287
[8] Harrison W A 1980 *Electronic Structure and the Properties of Solids* (New York: Freeman)
[9] Slater J C and Koster G F 1954 *Phys. Rev.* **94** 1498
[10] Baldereschi A, Hess E, Maschke K, Neumann H, Schulte K R and Unger K 1977 *J. Phys. C: Solid State Phys.* **10** 4709
[11] Lorenz M R and Onton A 1970 *Proc. 10th Int. Conf. on Semiconductor Physics (Cambridge, MA)* (New York: USAEC) p 444
[12] Nahory R E, Pollak M A and DeWinter J C 1975 *J. Appl. Phys.* **46** 775
[13] Hermann C and Weisbuch C 1977 *Phys. Rev.* B **15** 823
[14] Mikkelsen J C Jr and Boyce J B 1984 *Phys. Rev.* B **28** 7130
[15] Martins J L and Zunger A 1984 *Phys. Rev.* B **30** 6217
[16] Cai Y and Thorpe M F 1992 *Phys. Rev.* B **46** 15 879
[17] Wilke S and Hennig S 1991 *Phys. Rev.* B **43** 12 470
[18] Varfolomeev A V, Seisyan R P and Yakimova R N 1975 *Sov. Phys.–Semicond.* **9** 530 (Engl. Transl. 1975 *Fiz. Tekh. Poluprov.* **9** 804)
[19] Rochon P and Fortin E 1975 *Phys. Rev.* B **12** 5803
[20] Harrison W A 1977 *J. Vac. Sci. Technol.* **14** 1016
[21] Batey J and Wright S L 1986 *J. Appl. Phys.* **59** 200
[22] Yeh C N, McNell L E, Blue L J and Daniels-Race T 1995 *J. Appl. Phys.* **77** 4541
[23] Christensen N E 1988 *Phys. Rev.* B **37** 4528
[24] Lambrecht W R L and Segall B 1988 *Phys. Rev. Lett.* **61** 1764
[25] Nelson J S, Wright A F and Fong C Y 1991 *Phys. Rev.* B **43** 4908
[26] Wang Renzhi and Zheng Yongmei 1996 *Chinese J. Semicond.* **17** 161
[27] Böhrer J, Krost A, Wolf T and Bimberg D 1993 *Phys. Rev.* B **47** 6439
[28] Lang D V, Panish M B, Capasso F, Allam J, Hamm R, Sergent A M and Tsang W T 1987 *Appl. Phys. Lett.* **50** 736
[29] Aspnes D E and Studna A A 1973 *Phys. Rev.* B **7** 4605
[30] Pidgeon C R, Groves S H and Feinleib J 1967 *Solid State Commun.* **5** 677
[31] Hermann C and Weisbuch C 1977 *Phys. Rev.* B **15** 823
[32] Olego D, Chang T Y, Silberg E, Caridi E A and Pinczuk A 1982 *Appl. Phys. Lett.* **41** 476